Article

Underwater Hyperspectral Imaging of Arctic Macroalgal Habitats during the Polar Night Using a Novel Mini-ROV-UHI Portable System

Natalie Summers [1,*], Geir Johnsen [1,2], Aksel Mogstad [1], Håvard Løvås [3], Glaucia Fragoso [1] and Jørgen Berge [1,2,4]

1   Centre for Autonomous Marine Operations and Systems (AMOS), Trondheim Biological Station, Department of Biology, Norwegian University of Science and Technology (NTNU), 7018 Trondheim, Norway; geir.johnsen@ntnu.no (G.J.); aksel.a.mogstad@ntnu.no (A.M.); glaucia.m.fragoso@ntnu.no (G.F.); jorgen.berge@uit.no (J.B.)
2   Department of Arctic Biology, University Centre in Svalbard (UNIS), 9170 Longyearbyen, Norway
3   Centre for Autonomous Marine Operations and Systems (AMOS), Department of Marine Technology, Norwegian University of Science and Technology (NTNU), 7491 Trondheim, Norway; havard.s.lovas@ntnu.no
4   Faculty of Biosciences, Fisheries and Economics, Arctic University of Norway (UiT), 9037 Tromsø, Norway
*   Correspondence: natalie.summers@ntnu.no

Abstract: We describe an Underwater Hyperspectral Imager (UHI) deployed on an instrument-carrying platform consisting of two interconnected mini-ROVs (Remotely Operated Vehicle) for the mapping and monitoring of Arctic macroalgal habitats in Kongsfjorden (Svalbard) during the Polar Night. The mini-ROV-UHI system is easy to transport, assemble and deploy from shore, even under the dark, icy and cold conditions of the Arctic Polar Night. The system can be operated by two persons, keeping the operational costs low. In vivo hyperspectral reflectance of collected specimens of brown, red and green macroalgae was measured with a spectrometer in the lab to provide a spectral library for supervised pigment group classification based on UHI photomosaics. The in situ UHI-photomosaics provided detailed information of the areal coverage of the seafloor substrate (16%), as well as brown (51% habitat cover), red (18%), and green (14%) macroalgae, with spatial resolution in the range of cm and spectral resolution of 2 nm. The collected specimens from the mapped area were also used for species identification and health state evaluation. This innovative UHI sampling method provides significant information about macroalgal distribution and physiology, and due to its flexibility in terms of deployment, it is applicable to a variety of environments.

Keywords: underwater hyperspectral imaging (UHI); mini ROV (Remotely Operated Vehicle); in situ/in vivo spectral reflectance; underwater habitat mapping; Svalbard; arctic; phaeophytes; chlorophytes; rhodophytes; polar night

1. Introduction

The use of underwater hyperspectral imaging (UHI) was first published in 2013 [1,2] and first reviewed by [3,4], covering the use of UHI for the identification and mapping of different bio-geo-chemical Objects of Interest (OOI). UHI has been conducted from different instrument-carrying platforms, such as SCUBA diving [2,5] landers [6], underwater slides [1], remotely operated vehicles (ROV) operating from the surface and down to 4200 m [5,7–10], autonomous underwater vehicles (AUV) [11] and unmanned surface vehicles (USV), [12]. Aerial hyperspectral imaging of kelp forests in the Arctic was performed for the first time by using a two engine Dornier airplane carrying a prototype hyperspectral imager (HI) [13]. The airborne campaign was conducted in concert with kelp forest measurements (in situ spectral reflectance) in Kongsfjorden, May 2004 [13]. The current study with mini-ROV-UHI was conducted in the same area [13] in January

2020 during the Polar Night (Figure 1). However, these airborne methods (passive remote sensing) are limited by solar illumination (March to October in Kongsfjorden) making passive remote sensing impossible from November to February due to the Polar Night [14]. In addition, water clarity is low during summertime due to glacial run-off of particles and phytoplankton blooms [13,15], restricting reflected light from macroalgae to be detected by aerial remote sensing. In contrast, during the Polar Night, in situ mapping is restricted to active remote sensing using artificial light sources, which has not been achieved previously.
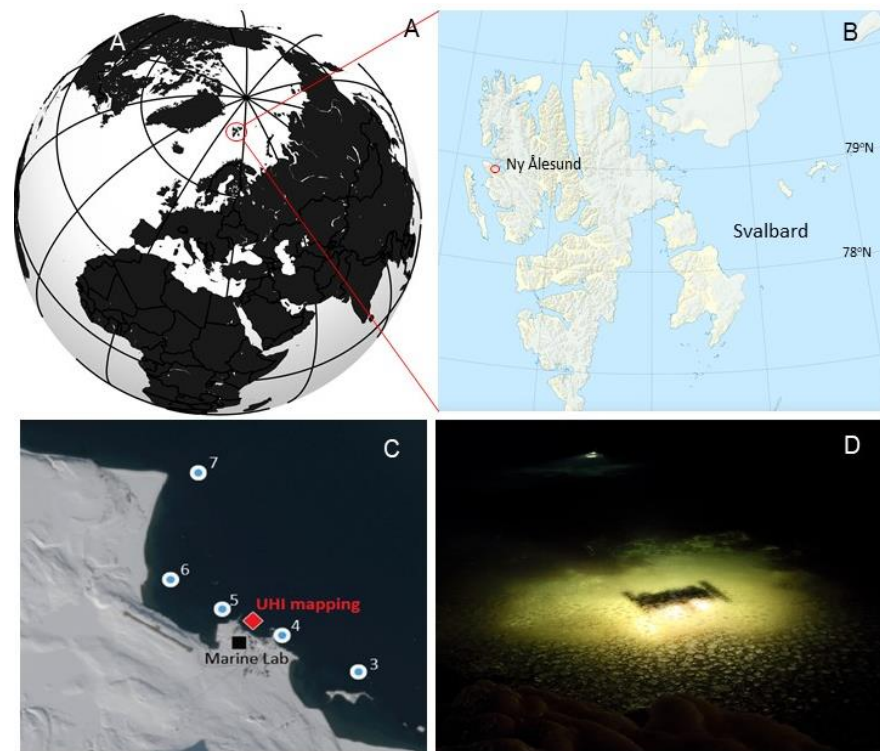

Figure 1. (**A**,**B**) Geoposition of Svalbard. (**C**) The ROV-UHI study site outside the Marine Lab, Ny Ålesund in Kongsfjord. Current UHI survey site (red diamond) in front of the Marine Lab (black square). Aerial hyperspectral imaging study sites from [13] are shown as blue points (3–7). (**D**) ROV-UHI underneath pancake ice. Credits: (**A**,**B**) based on [14]; (**C**) N. Summers (modified from https://geokart.npolar.no/, accessed 16 September 2022) and (**D**) N. Summers.

Macroalgal systematics in Kongsfjorden during the summer season have previously been reviewed [16]. A review of the light regime during the summer season in air and water was carried out by [17]. Polar Night macroalgal biodiversity, ecology, and environmental variables from Kongsfjorden have been reviewed by [15]. Knowledge about macroalgal dynamics (presence, composition, health state) during the three months of Polar Night darkness remains limited to a few species of brown algae [15]. Ecologically relevant light regime data (intensity, spectral composition, and day length), the most important environmental variable for photosynthetic organisms, was provided from the ArcLight observatory in Kongsfjorden for 2017–2020, with 1 h temporal resolution [14].

Fast, precise, and affordable approaches for the identification, mapping and monitoring of marine habitats are needed to provide knowledge and information for nature management and policy-making decisions in marine environments [7]. In situ sampling and mapping of seabed natural communities involving divers, ship-based acoustics, box corers, trawls, RGB photography and video are usually spectrally limited [4]. Satellite-based ocean colour techniques only cover surface waters, while information from the deep habitats is missing.

With the double mini-ROV system described here, we were able to map a macroalgal habitat with a spatial resolution in the range of centimetres with a corresponding spectral

resolution of 2 nm. Because our system (double mini-ROV with the UHI attached) is light (35 kg), it does not require large research vessels and deployment is possible from land or from a small boat. As the system is developed towards becoming more autonomous, the spatial range of data collection will increase from tens of meters to hundreds of meters. By being successful in creating maps in extreme areas, such as during the Arctic Polar Night with dark, cold and icy conditions, this system should also work elsewhere, globally, in less hostile environments [18].

This paper describes a double, interconnected mini-ROV system, comprising a UHI, a battery-powered light source, and an altimeter (estimation of distance between UHI and seafloor) for the identification, mapping and monitoring of seafloor habitats. The ROV-UHI unit comprises two mini-ROVs and a UHI, which can easily be disassembled into three boxes (volume of mid-size suitcases) for transport by car, boat, or airplane and quickly assembled in the field. We describe a battery-powered mini-ROV-UHI system to create useful habitat maps in extreme conditions of the Arctic Polar Night when other methods are limited due the dependence on solar illumination and large robotic systems requiring expensive logistics.

2. Materials and Methods

2.1. Study Area

The study was carried out at 1–2 m depth along the coastal line outside the Marine Laboratory in Ny-Ålesund, Kongsfjorden, Spitsbergen (78°55′40.0″ N 11°55′52.9″ E) on the 11–12 January 2020 (Figure 1). The macroalgal habitat was dominated by the kelp species *Saccharina nigripes* (often indicated as *Laminaria digitata*, see discussion of this species complex in [16]), *Saccharina latissima* and *Alaria esculenta*. The seabed was characterised by a rocky bottom and coarse sand covered by three major macroalgal pigment groups belonging to algal classes Phaeophyceae (brown algae), Chlorophyceae (green algae) and Rhodophyceae (red algae), detailed in [15,16]. Ice-scouring of macroalgae was observed in the shallowest parts close to shore. During the mapping survey, the weather was calm (air temperature −15 °C to −20 °C) with corresponding water temperatures of −1.8 °C, resulting in the formation of pancake ice on the surface, Figure 1D).

2.2. Mini ROV Platform as UHI Carrier

The overall line-up of the interconnected mini-ROVs-UHI system is detailed in [19] and has a total weight in air of 35 kg. Each Blueye Pioneer ROV (Blueye AS, Trondheim, Norway) weighs 9 kg in air, and is able to carry the underwater hyperspectral imager UHI-4 (Ecotone AS, Trondheim, Norway) that also weighs 9 kg in air (Figure 2). The ROV has a 96 Wh lithium-ion smart battery, avoiding the need for a "Dangerous Goods Declaration" (DGD) for air transport (DGD needed for lithium batteries > 100 Wh). The battery time was 2 h at 20 °C but reduced by 50% due to the cold conditions in which they were used (−15 °C air temperature and −1.8 °C water temperature).

The UHI was connected to an underwater electronic housing (Figure 2 #4) containing the UHI battery and a Raspberry Pi computer. The UHI typically consumed 20 W with a maximum of 35 W (UHI-4 manual, Ecotone AS). The electronic housing and the two ROVs were then connected to a surface modem through a "twisted pair" tether containing two wires to transmit and receive data. We then used Wi-Fi to communicate from the modem to a Dell field laptop connected to a power source from the Marine Lab. The UHI captured images using a scientific complementary metal-oxide-semiconductor (sCMOS) camera sensor with a 12-bit radiometric resolution (dynamic range) through an 8 mm fore lens providing a field of view of 60° (transversal) and 0.4° (longitudinal). The spatial resolution of the spectrograph camera was 1936 spatial pixels (image slit) with a spectral resolution of 0.5 nm in the range of 380–750 nm. Prior to providing the UHI transect line, the spectral and spatial binning was set to 2 nm and 968 pixels, respectively, through Ecotone's "Immersion" UHI software (Ecotone AS, Trondheim, Norway). We used a 105 W Keldan Video 8 M CRI LED (light- emitting diode) lamp (KELDAN GmbH, Brügg, Switzerland) to provide

"broadband white light", optimized for underwater imaging. The light was mounted facing down on the aft of the ROV, providing even seafloor illumination using a 90° diffuser for 50 min at full capacity (Figure 3). One person operated the UHI acquisition by using the "Immersion" software, while another operator controlled the ROV via a gamepad that communicated with the field laptop through Bluetooth.
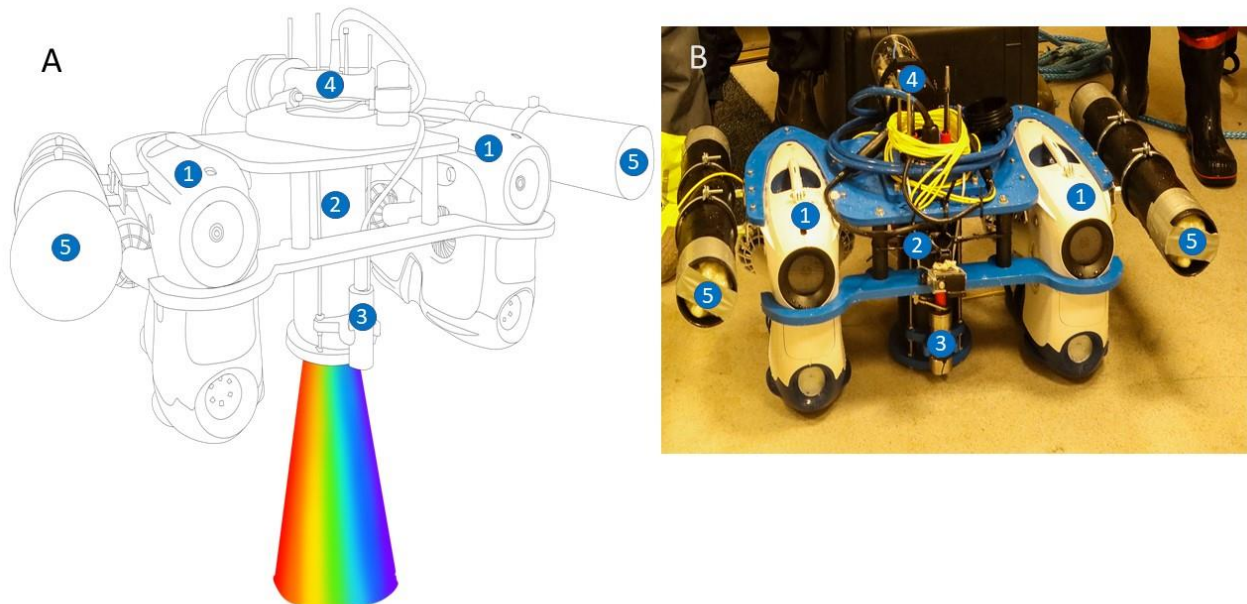

Figure 2. (**A**) Schematic front view of the double mini-ROV rig used (Blueye Pioneer, Blueye), as a carrier for an Underwater Hyperspectral Imager (UHI-4, Ecotone). 1. Mini-ROV, 2. UHI, 3. Altimeter, 4. Underwater electronic housing, 5. Buoyancy tubes (PVC tubes filled with incompressible foam). (**B**) Front view of the mini-ROV rig. Credits: (**A**) by Malin Bø Nevstad, (**B**) by Geir Johnsen.
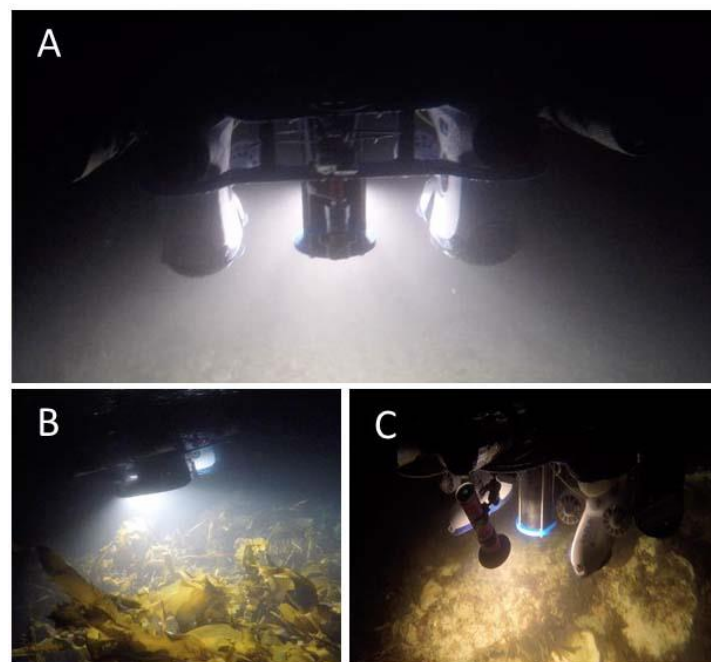

Figure 3. In situ images of mini-ROV UHI survey. (**A**) Front view of ROV-UHI rig showing illumination from lamp during kelp forest mapping. (**B**) Side view of the mini-ROV-UHI over the kelp forest habitat during the transect. (**C**) Aft view of ROV with lamp and UHI over the seafloor. Credits: (**A**–**C**) by Geir Johnsen.

There was no global positioning on the vehicle (and the magnetic compass gave faulty measurements due to closeness to the magnetic North pole). Navigation was, therefore, conducted manually using visual landmarks to assess heading and speed. For data processing purposes, we assume that the ROV track was a straight line moving at a constant speed and heading. An acoustic altimeter measured the altitude from the seafloor (below the macroalgae). Lastly, we used the altitude with the flat seabed assumption for estimating the position of measurements across-track. The main transect line was estimated to be 28 m in length and the vehicle had a constant depth control at 0.5 m depth with an altitude to the seafloor varying between 0.6–1.5 m. The ROV-UHI transect speed was estimated to be 0.3 m s^{-1} based on 3 min for a 60 m transect.

At the beginning of each transect, the UHI was scanning over a Spectralon reflectance standard (SRT-99-050 from Labsphere Inc., North Sutton, USA, providing 99% light reflection from 400–700 nm) placed in an open seafloor area. Given multiple measurements of the Spectralon at varying distances, we estimated the normalized spectral light beam attenuation, $c(\lambda)$. Immersion software converted the UHI data to absolute radiance. Furthermore, all radiance spectra were normalized by the radiance at 574 nm (high signal-to-noise ratio) to remove baseline effects (wavelength-independent effects) and converted to reflectance taking into account inherent optical properties (IOP) and light source spectra using the following Equation (1) [20]. Each UHI-based pixel has reflectance spectra that can be compared to the lab-based reflectance spectra for classification.

$$R(\lambda)= [L_{u\ OOI}\ (\lambda)]/L_0\ (\lambda)] \times e^{(2c(\lambda)(d-d_0))} \tag{1}$$

where: R: Normalised spectral reflectance, $L_{u\ OOI}$: Normalized in situ upwelling radiance measurement of the OOI; L_0: Normalized in situ radiance measurement of reflectance standard at distance d_0; $c(\lambda)$: Normalized light beam attenuation coefficient; d: Distance to OOI.

2.3. Classification of UHI Data

After optical corrections described above and geometrical correction based on the pitch and roll of the mini ROV [19], the UHI-based reflectance spectra were classified using a two-step classification procedure. The first step was applying the spectral angle mapper (SAM) algorithm based on the spectral library of macroalgal reflectance spectra (green, red and brown macroalgae) measured in the lab beforehand. The spectral library also featured reflectance spectra of various minerals/rocks), as well as coralline algae and calcium carbonate covered in green-algal biofilm. The SAM classification was performed within the spectral interval of 490–690 nm using a narrow maximum angle threshold of 0.09 radians. The interval of 490–690 nm was chosen to eliminate wavelengths with low signal-to-noise ratio in parts of the recorded UHI data, whereas the narrow maximum angle threshold was chosen to make sure only pixel spectra very closely resembling a library spectrum were classified [1].

In the second step, pixels identified by the SAM algorithm were extracted and used as training data for a full-scale Support Vector Machine (SVM) classification with a radial basis function kernel [1]. SVM was chosen due to its previous performances with UHI data [7–10,12]. The training data were categorized into four classes based on their spectral signatures: (1) green algae (green algae and calcium carbonate covered with green alga-like biofilm), (2) red algae (leafy red algae and coralline red algae), (3) brown algae and (4) substrate (different minerals). The classifier was tuned using ten-fold cross-validation, which found that a γ (kernel width) of 10^{-6} in combination with a C (regularization degree) of 10^6 yielded the best classification results (100% cross-validation accuracy). Ultimately, the tuned SVM classifier was applied to the full UHI dataset, yielding a macroalgal map of the survey area. The spectral classification was carried out in the software application ENVI (Environment for Visualizing Images, v. 5.6; Harris Geospatial Solutions Inc., Broomfield, CO, USA), while the SVM tuning was performed in the software environment R, using the package "e1071" [21].

2.4. Ground-Truthing

Two snorkelers collected three specimens of each of the seven most common macroalgal species (Figure 4). Chlorophyceae: *Ulva sp.*, Rhodophyceae: *Palmaria palmata*, Phaeophyceae: *Laminaria digitata/S. nigripes*, *Alaria esculenta*, *Saccharina latissima*, *Fucus distichus*, and *Desmarestia aculeata*. The samples were kept in nets on site at approximately 2 m depth during sampling and stored in 10-L plastic buckets of freezing seawater in a cold room (4 °C) on board until they were processed.

A QE Pro spectrometer (Ocean Insight Inc., Orlando, FL, USA), equipped with an HL-2000-HP high-power tungsten halogen light source from Ocean Insight Inc. (Ocean Insight Inc., Orlando, FL, USA) was used to measure in vivo reflectance spectra between 400 to 700 nm on subsamples from new and old tissue of each macroalgal specimen. The reflectance was measured using a QR 400-7-VIS-BX reflection probe with optical fibres (Ocean Insight Inc., Orlando, FL, USA) and was normalized to a white WS-1 reflectance standard (Ocean Insight Inc., Orlando, FL, USA). Live specimens were also used for photosynthesis measurements and the tissues were frozen in −80 °C for High Performance Liquid Chromatography (HPLC) analysis of pigments (in prep).

Figure 4. The 8 major macroalgal species sampled from Kongsfjorden macroalgal habitat in January 2020. (**A**) Chlorophyte *Ulva* sp.; (**B**) Rhodophytes *Palmaria palmata*; (**C**) unknown Rhodophyte. (**D–H**) Phaeophytes: (**D**) *Fucus distichus*, (**E**) *Laminaria digitata*, (**F**) *Saccharina latissima*, (**G**) *Desmarestia aculeata* and (**H**) *Alaria esculenta*.

3. Results

The in vivo reflectance spectra, R(λ), of collected macroalgae, measured in the laboratory reflected the pigment signatures from three macroalgal classes (herein referred to as "pigment groups", Figure 5). High pigment absorption was observed as low R(λ) at 650 nm (chl b) and 677 nm for green algae, 530–570 nm (phycoerythrin) and 680 nm (chl a) for red algae and 535 nm (fucoxanthin), 630 nm (chl c) and 674 nm (chl a) for brown algae (Figure 5).

Using the reflectance data, the spectra from the hyperspectral images of the seafloor habitat were classified into 4 categories: green, red and brown algae and substrate (minerals). Minerals covered 16.06%, red algae 18.14%, green algae 14.10% and brown algae 51.70% of the UHI transect (Figure 5). Verification (ground-truthing) of collected specimens confirmed the correct identification of algal group and indicated that the estimation of algal cover was accurate (Figure 5).
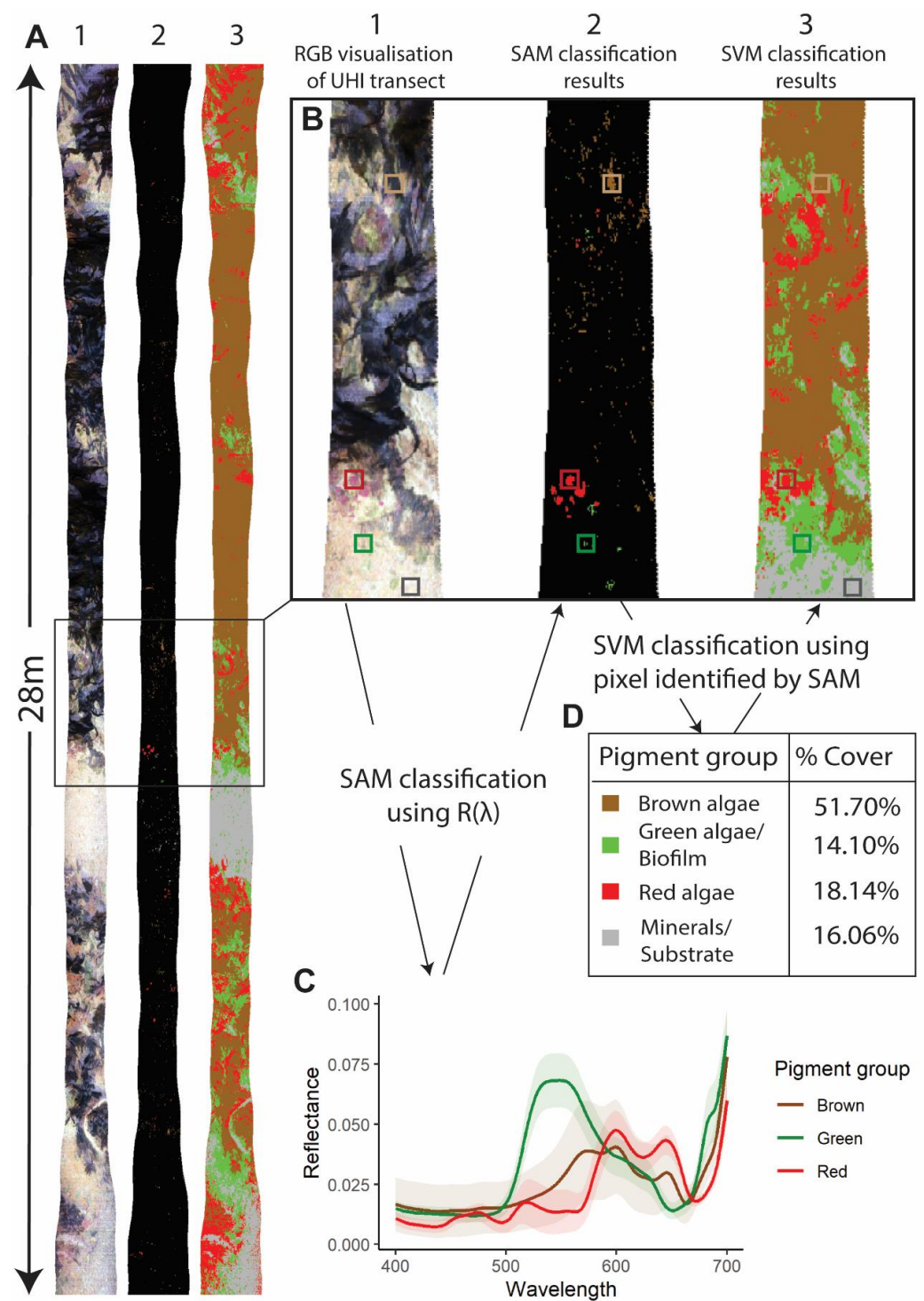
Figure 5. (**A**,**B**) Stages (1–3) for making a map of the macroalgal habitat. Stage 1, RGB visualisation of the UHI transect; Stage 2, Application of spectral angle mapper (SAM) algorithm based on the spectral library of brown, red and green macroalgal in vivo reflectance spectra taken in the lab (**C**); Stage 3, Support Vector Machine (SVM) classification of all remaining pixel into green, brown, red macroalgae and substrate using from SAM pixels as training data. (**C**) In vivo reflectance spectra (R(λ)) with standard error of the mean for each pigment group, measured with a spectrometer. Low R(λ) indicates high absorption at 650 nm (chl b) and 677 nm for green algae, 530–570 nm (phycoerythrin) and 680 nm (chl a) for red algae and lastly 535 nm (fucoxanthin), 630 nm (chl c) and 674 nm (chl a) for brown algae. (**D**) Percent areal cover of each OOI.

4. Discussion

4.1. ROV-UHI Macroalgal Habitat Mapping during the Polar Night

We here report a novel ROV-UHI-survey indicating that the majority of brown, green and red macroalgal species were healthy during the Polar Night. This was indicated by appearance (Figure 4), in vivo R(λ) (showing major functional pigment absorption signature of all pigments, Figure 5), absence of degraded pigments evident in all tissues (HPLC, in prep) and the 8 major species were also able to perform photosynthesis when artificial actinic light was provided (Pulse Amplitude Modulated fluorometry, in prep). The mapped macroalgal habitat in Kongsfjorden was dominated by the brown algae, *Laminaria digitata*, *Alaria esculenta*, *Saccharina latissima, Fucus distichus*, and *Desmarestia aculeata*, covering 51.70% of the examined area. The corresponding red and green algal cover comprised 18% and 14% of the mapped area, respectively (Figure 5).

Our study strongly indicates that many algal species, comprising red, green and brown algae, thrived during the dark period (Polar Night). The 8 species examined survived and thrived for >3 months under an irradiance far below the limits for photosynthetic activity (actinic light). Actinic light is generally defined as percent hours per month (H%) with downwelling irradiance higher than 0.01 μmol m^{-2} s^{-1} [14]. The actinic light in Kongsfjorden increases very rapidly in February and March reaching 100 H% in April-August (midnight sun) [14]. Previous studies have shown that the brown algal species *Laminaria solidungula* and *S. latissima* can survive during the Polar Night [15].

The double mini-ROV system presented provides a stable UHI carrier which is easy to transport (35 kg and small size), can be used and deployed from shore by 2 persons and can be disassembled and reassembled. Other ROV systems carrying an UHI typically weigh between 250 kg (inspection ROV, [5,10]) and 3500 kg (work class ROV, [9]). We deployed the system in a water temperature of −1.8 °C with pancake ice forming on the surface. At the surface, the pancake ice interfered with the ROV thrusters creating air bubbles and ice particles resulting in blurry images. To avoid this problem, we operated the ROV from 10 to 50 cm below the surface. The buoyancy tubes (Figure 2 #5) enhance the buoyancy control and stability of the ROV in ice-free water surfaces and at discrete depths. Seeing the live feed (real-time) UHI (data collection) and RGB video acquisition from the ROV (navigation purposes) during our survey was important and was required for online adjustments, such as ROV speed, illumination, altitude to seafloor. The current system's ROVs had about 1 h operational time in these cold conditions. However, the battery packs are easily replaceable without dissembling the whole set-up. The current system is fully manually controlled. Future updates will include automated depth, speed and heading control. This will facilitate route planning, resulting in a more systematic approach to underwater mapping. This study is a proof-of-concept of the mini-ROV-UHI for mapping and monitoring macroalgal habitats in the Arctic. In addition, the system allows us to gather data during the Polar Night when the dark and icy conditions limit the use of other instrument-carrying platforms (such as satellites, airplanes, drones and USV).

During the Polar Night, the water column is usually quite clear, which is optimal for seafloor imaging. High water transparency is caused by low phytoplankton biomass (<0.01 mg chl a m^{-3}), low concentration of coloured dissolved organic matter (cDOM) and total suspended matter (TSM) [15].

There were several factors that affected the in situ reflectance signal of the macroalgae, primarily the distance between the algae and the UHI. The effect of the inherent optical properties (IOP) of the water caused by the absorption and scattering properties of phytoplankton, cDOM and TSM causes variance in the intensity and shape of the spectral signal of the macroalgae and water properties [1]. This potential variation in the IOPs may be higher than the variability of bio-optical properties between species of the same macroalgae pigment group. As a result, we were not able to distinguish between species of the same pigment class.

Another challenge with in situ mapping of macroalgae habitats is that thallus and lamina of larger species (especially kelp) are constantly moving due to wave action and

tidally driven currents. Although the movement did not create any issue regarding the image quality in our study, the fact that the orientation and movement of the lamina were constantly changing during imaging may have introduced errors in the UHI-based percent areal cover estimates. This is especially evident with large kelp species, which have a lamina length that can extend up to 5 m in this area, often twisted and swaying (due to current and swell) in the macroalgal habitat [15,16]. For smaller species, such as wrack (brown algae), red and green algae, this is not a major issue compared to the large kelp species.

4.2. In Vivo Bio-Optical Characteristics of Macroalgae

The shape of the in vivo R(λ) and its intensity (related to pigment concentration in tissue) were used to estimate underwater coverage of brown, red and green macroalgae [15]. Both in situ and in vivo laboratory R(λ) on collected algal specimens indicated the major pigments found in the brown, red and green macroalgae (Figures 4 and 5).

Brown algae is distinguished from the green and red algae by the presence of chl c with peak absorption at 460 nm and minor peaks at 585 and 635 nm [22]. These chromophytes (chl c-containing algae) also contain fucoxanthin that has distinct absorption shoulders at 480, 520 and 545 nm [22].

Red algae are mainly distinguished from brown and green algae by the presence of the phycobiliprotein phycoerythrin that absorbs between 500–600 nm. These absorption peaks are detected as dips in the reflectance data, indicating the corresponding high absorption by pigments (Figure 5C). Figure 5B shows that the SAM algorithm classified coralline algae in the red algae class with *P. palmata* due to similar R(λ) related to their pigment composition [8,15].

The green algae were characterized by the absorption peaks (or reflectance dip) corresponding to the following pigments: chl a, chl b and lutein. This is seen by in vivo R(λ) dips at 400–500 nm due to all major pigments of green algae, and at 650 nm due to chl b (Figure 5). Our findings regarding optical fingerprints from R(λ) from in situ and in vivo specimens are in agreement with in vivo absorption properties of the same macroalgal groups found in the Trondheim fjord, Norway [15,22], where leafy green algae such as *Ulva* spp. are characterized by the major pigments chl a, chl b and lutein. For green algae, chl a has absorption peaks in vivo at 440 nm, 630 nm and 675 nm. Chl b has in vivo absorption peaks at 470 nm, 600 nm and 650 nm and the carotenoid lutein has an in vivo absorption peak at 460 nm and 485 nm [22]. The indication of green algae, seen as reflectance of biofilm-like structures, is likely caused by the chl b. Biofilms are important to the ecosystem, providing food to other organisms and potentially "seeds" for micro- and macroalgae when light becomes available in the spring [15]. Future research on this topic could offer important insights on biofilm composition and the role of algal dynamics in the Arctic.

5. Conclusions

The UHI has shown potential for the identification of macroalgal groups that are hard to see or identify with the human eye or with an RGB camera (such as coralline algae and biofilm). In addition, the optical correction described here (Equation (1)) allowed us to classify pixels directly based on in vivo reflectance signatures. This automated classification, using spectral fingerprints to classify individual pixels, greatly reduces the time needed to create maps of OOI. The maps created by the UHI can be a base to select areas of interest for more detailed experiments.

The relatively small size and weight of this ROV and UHI system may reduce the user threshold and cost for mapping of seafloor and facilitate the logistics for field work in remote areas. Future improvement of the software can make the navigation system more autonomous and able to follow a survey pattern. Currently, work with additional IOP sensors will allow us to correct for spectral attenuation of constituents of seawater itself and its optical active constituents to improve the OOI signatures. The current use of the acoustic altimeter gave us the ability to stay at a fixed depth. Ongoing work to estimate the

distance from the instrument-carrying robot to the habitat/OOI is challenging in a kelp forest due to the movement of macroalgae caused by waves and currents. This challenge may be solved by other types of non-acoustic altimeters based on optics, such as Lidars.

We have shown that our innovative ROV-UHI rig can function in extreme conditions of the Polar Night, at −2 °C water temperature and under sea-ice formation. The setup is simple to transport, making it ideal for in situ OOI identification, mapping and monitoring. Thus, the system should work with great ease in less hostile environments around the globe. Future updates will include enhanced altitude control (distance from the seafloor or other surface), more automated navigation, and heading control and speed control, making the system more versatile. These in situ hyperspectral habitat maps, using UHI as an active remote sensing sensor (equipped with its own light source), provide data when airborne platforms cannot, such as when there is a lack of ambient light, cloud cover or for deeper seafloor mapping. In addition, the data collected can be used to verify/ground truth remotely sensed RGB-, multi- or hyperspectral images collected from these airborne platforms.

Author Contributions: Conceptualization, N.S., G.J., A.M. and H.L.; Formal analysis, N.S., A.M. and H.L.; Funding acquisition, G.J. and J.B.; Investigation, N.S., G.J., A.M. and H.L.; Methodology, N.S., G.J., A.M. and H.L.; Project administration, G.J. and J.B.; Supervision, G.J. and G.F.; Visualization, N.S., G.J. and A.M.; Writing—original draft, N.S.; Writing—review and editing, N.S., G.J., A.M., H.L., G.F. and J.B. All authors have read and agreed to the published version of the manuscript.

Conflicts of Interest: The authors declare no conflict of interest. The funders had no role in the design of the study; in the collection, analyses, or interpretation of data; in the writing of the manuscript, or in the decision to publish the results.

References

1. Johnsen, G.; Volent, Z.; Dierssen, H.; Pettersen, R.; Van Ardelan, M.; Søreide, F.; Fearns, P.; Ludvigsen, M.; Moline, M. Underwater hyperspectral imagery to create biogeochemical maps of seafloor properties. In *Subsea Optics and Imaging*; Woodhead Publishing: Sawston, UK, 2013; pp. 508–535; ISBN 9780857093417.
2. Chennu, A.; Färber, P.; Volkenborn, N.; Al-Najjar, M.A.A.; Janssen, F.; de Beer, D.; Polerecky, L. Hyperspectral imaging of the microscale distribution and dynamics of microphytobenthos in intertidal sediments. *Limnol. Oceanogr. Methods* **2013**, *11*, 511–528. [CrossRef]
3. Liu, B.; Liu, Z.; Men, S.; Li, Y.; Ding, Z.; He, J.; Zhao, Z. Underwater Hyperspectral Imaging Technology and Its Applications for Detecting and Mapping the Seafloor: A Review. *Sensors* **2020**, *20*, 4962. [CrossRef] [PubMed]
4. Montes-Herrera, J.C.; Cimoli, E.; Cummings, V.; Hill, N.; Lucieer, A.; Lucieer, V. Underwater hyperspectral imaging (UHI): A review of systems and applications for proximal seafloor ecosystem studies. *Remote Sens.* **2021**, *13*, 3451. [CrossRef]
5. Johnsen, G.; Ludvigsen, M.; Sørensen, A.; Sandvik Aas, L.M. The use of underwater hyperspectral imaging deployed on remotely operated vehicles—methods and applications. *IFAC-PapersOnLine* **2016**, *49*, 476–481. [CrossRef]
6. Dumke, I.; Ludvigsen, M.; Ellefmo, S.L.; Søreide, F.; Johnsen, G.; Murton, B.J. Underwater Hyperspectral Imaging Using a Stationary Platform in the Trans-Atlantic Geotraverse Hydrothermal Field. *IEEE Trans. Geosci. Remote Sens.* **2019**, *57*, 2947–2962. [CrossRef]
7. Johnsen, G.; Mogstad, A.A.; Berge, J.; Cohen, J.H. Operative habitat mapping and monitoring in the polar night. In *Polar Night Marine Ecology: Life and Light in the Dead of Night*; Berge, J., Johnsen, G., Cohen, J.H., Eds.; Springer International Publishing: Cham, Switzerland, 2020; pp. 277–305; ISBN 978-3-030-33208-2.
8. Mogstad, A.A.; Johnsen, G. Spectral characteristics of coralline algae: A multi-instrumental approach, with emphasis on underwater hyperspectral imaging. *Appl. Opt.* **2017**, *56*, 9957. [CrossRef]
9. Dumke, I.; Nornes, S.M.; Purser, A.; Marcon, Y.; Ludvigsen, M.; Ellefmo, S.L.; Johnsen, G.; Søreide, F. First hyperspectral imaging survey of the deep seafloor: High-resolution mapping of manganese nodules. *Remote Sens. Environ.* **2018**, *209*, 19–30. [CrossRef]
10. Ødegård, Ø.; Mogstad, A.A.; Johnsen, G.; Sørensen, A.J.; Ludvigsen, M. Underwater hyperspectral imaging: A new tool for marine archaeology. *Appl. Opt.* **2018**, *57*, 3214. [CrossRef] [PubMed]

11. Sture, Ø.; Ludvigsen, M.; Søreide, F.; Aas, L.M.S. Autonomous underwater vehicles as a platform for underwater hyperspectral imaging. In Proceedings of the OCEANS 2017, Aberdeen, UK, 19–22 June 2017; pp. 1–8.

12. Mogstad, A.A.; Johnsen, G.; Ludvigsen, M. Shallow-water habitat mapping using Underwater Hyperspectral Imaging from an Unmanned Surface Vehicle: A pilot study. *Remote Sens.* **2019**, *11*, 685. [CrossRef]

13. Volent, Z.; Johnsen, G.; Sigernes, F. Kelp forest mapping by use of airborne hyperspectral imager. *J. Appl. Remote Sens.* **2007**, *1*, 011503. [CrossRef]

14. Johnsen, G.; Zolich, A.; Grant, S.; Bjørgum, R.; Cohen, J.H.; McKee, D.; Kopec, T.P.; Vogedes, D.; Berge, J. All-sky camera system providing high temporal resolution annual time series of irradiance in the Arctic. *Appl. Opt.* **2021**, *60*, 6456. [CrossRef] [PubMed]

15. Johnsen, G.; Leu, E.; Gradinger, R. Marine micro- and macroalgae in the polar night. In *Polar Night Marine Ecology: Life and Light in the Dead of Night*; Berge, J., Johnsen, G., Cohen, J.H., Eds.; Springer International Publishing: Cham, Switzerland, 2020; pp. 67–112; ISBN 978-3-030-33208-2.

16. Fredriksen, S.; Karsten, U.; Bartsch, I.; Woelfel, J.; Koblowsky, M.; Schumann, R.; Moy, S.R.; Steneck, R.S.; Wiktor, J.M.; Hop, H.; et al. Biodiversity of benthic macro- and microalgae from svalbard with special focus on kongsfjorden. In *The Ecosystem of Kongsfjorden, Svalbard*; Hop, H., Wiencke, C., Eds.; Springer International Publishing: Cham, Switzerland, 2019; pp. 331–371; ISBN 978-3-319-46425-1.

17. Pavlov, A.K.; Leu, E.; Hanelt, D.; Bartsch, I.; Karsten, U.; Hudson, S.R.; Gallet, J.-C.; Cottier, F.; Cohen, J.H.; Berge, J.; et al. The underwater light climate in Kongsfjorden and its ecological implications. In *The Ecosystem of Kongsfjorden, Svalbard*; Hop, H., Wiencke, C., Eds.; Springer International Publishing: Cham, Switzerland, 2019; pp. 137–170; ISBN 978-3-319-46425-1.

18. Sørensen, A.J. Testination north. In *Whither the Arctic Ocean? Research, Knowledge Needs and Development en Route to the New Arctic*; Paul, W., Ed.; Fundacion BBVA: Bilbao, Spain, 2021; pp. 165–175; ISBN 978-84-92937-82-0.

19. Lovas, H.S.; Sorensen, A.J.; Ludvigsen, M. Framework for combining multiple lightweight underwater vehicles into super underwater vehicle. In Proceedings of the 2020 IEEE/OES Autonomous Underwater Vehicles Symposium (AUV), St. Johns, NL, Canada, 30 September–2 October 2020. [CrossRef]

20. Lovas, H.S.; Mogstad, A.A.; Sorensen, A.J.; Johnsen, G. A Methodology for Consistent Georegistration in Underwater Hyperspectral Imaging. *IEEE J. Ocean. Eng.* **2021**, 1–19. [CrossRef]

21. Meyer, D.; Dimitriadou, E.; Hornik, K.; Weingessel, A.; Leisch, F. e1071: Misc Functions of the Department of Statistics, Probability Theory Group (Formerly: E1071). TU Wien. R Package Version 1.7-1. Available online: https://CRAN.R-project.org/package=e (accessed on 31 January 2022).

22. Grzymski, J.; Johnsen, G.; Sakshaug, E. The significance of intracellular self-shading on the biooptical properties of brown, red, and green macroalgae. *J. Phycol.* **1997**, *33*, 408–414. [CrossRef]